EUROGRAPHICS Workshop on Graphics and Cultural Heritage (2017)
T. Schreck and T. Weyrich (Editors)

Towards Semi-Automatic Scaling Detection on Flat Stones

I. Muñoz-Pandiella[1,2,3], K. Akoglu[1], C. Bosch[4] and H. Rushmeier[1]

[1] Yale University, USA
[2] ViRVIG Research Center, Universitat de Girona, Spain
[3] XLIM Research Institute - CNRS, Université de Limoges, France
[4] Eurecat, Centre Tecnològic de Catalunya, Spain

Abstract

In Cultural Heritage projects, it is very important to identify and track weathering effects on monuments in order to design and test conservation strategies. Currently, this mapping is manual work performed by experts based on what they observe and their experience. In this paper, we present a workflow to map the weathering effect known as "scaling" on monuments with very little user interaction. First, we generate a 3D model of the monuments using photogrammetry techniques. Then, we reduce the noise in the acquired data using an adaptive and anisotropic filter. After that, we estimate the original shape of the surface before the weathering effects using the RANSAC algorithm. With this information, we perform a geometrical analysis to detect the features affected by this weathering effect and compute their characteristics. Then, we map the regions that have suffered scaling using the detected features and a segmentation based on the distance between the mesh and the unweathered surface. Our technique results can be very useful to understand the level of weathering of a monument and to trace the weathered parts through time automatically.

CCS Concepts

•***Computing methodologies*** → ***Shape analysis;*** *Mesh geometry models;* •***Human-centered computing*** → *Scientific visualization;*

1. Introduction

Stone is generally considered to be one of the most durable materials. Nonetheless, it is susceptible to deterioration. In fact, processes that are operating on site appear as deterioration patterns. They are the visible component of the decay which is a result of the interaction between the materials' intrinsic components (chemical, physical and physico-mechanical properties together with mineralogical and petrographic characteristics) and/or extrinsic factors (environmental conditions, anthropogenic factors etc.). Decay patterns provide information in relation to decay mechanisms. In most cases these mechanisms come from a group of processes i.e., physical, chemical and biological processes, that alter the physical and chemical state of materials in atmospheric conditions. Those processes may work individually, sequentially or simultaneously. In weathering studies the emphasis should be given to relationships between processes, weathering forms, material properties and environmental conditions. Holistic weathering research that includes intrinsic and extrinsic influences is vital for the better understanding of decay mechanisms. The deterioration patterns and their depiction on measured drawings are essential tools for the conservation scientist to work with, and constitute the basic units to define the relationships between the weathering types and the decay mechanisms.

Mapping of Visual Weathering forms is an established non-destructive procedure for in situ studies on materials damage and provides relevant information on the evolving decay mechanisms. However, they are not the only signatures of those processes. To support more consistent diagnostics complementary data is required. This data helps in assessing the present damage, the damage to appear in the near future and the undamaged parts of the building materials. Therefore, priority measures such as which parts are to be conserved first and more intensively can be developed with the help of maps of visual weathering types.

There are various descriptive schemes for the classification of weathering features on stone, most of which provide a framework for mapping the extent and nature of deterioration [WCTS03] [SP07]. One of the tasks of the ICOMOS ISCS has been to collect and combine the definitions that are in use for the visual weathering forms of stone to obtain a generalized glossary together with its translation to different languages during the last decades. While the "Illustrated Glossary of Stone Deterioration Patterns" [ICO08] of ICOMOS ISCS gives the explanations for different types of visual weathering types the assessments involve a high level of detailed surveying which leads to considerable demands on time and expertise. Moreover, the fact that the mapping process is based on observation and that it is a manual work, carries the possibility of getting different mappings for the same monuments. This possible disparity makes it difficult to track the weathering effects over time

DOI: 10.2312/gch.20171291

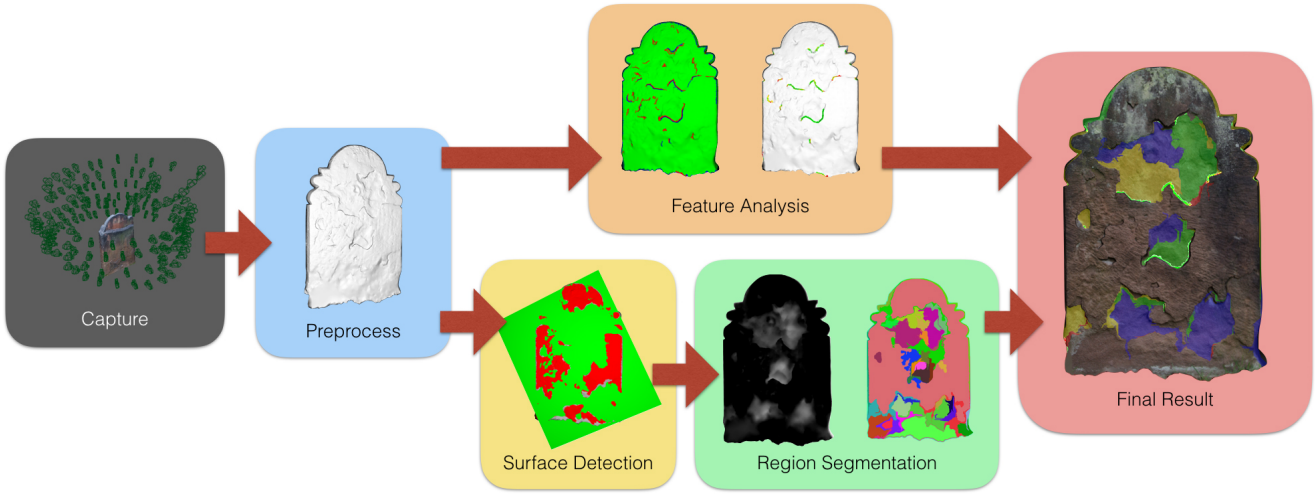

Figure 1: *Overview of our technique: First, we capture an scene using photogrammetry and we generate the corresponding 3D model. Then, we smooth this model in a preprocess in order to reduce acquisition noise. After that, on one hand, we perform a geometrical analysis to identify the features related to scaling weathering effect. On the other hand, we estimate the unweathered surface and we segment model regions according to their distance to it. Finally, we map the weathered zones on the model using the obtained segmentation and the detected weathering features.*

and to compare monitoring of the same monument made by different people.

In this work we focus on the weathering effect known as "scaling". Following the ICOMOS definition, we consider scaling the decay effect where there is a detachment of a stone as a scale or a stack of scales, not following any stone structure and detaching either as fish scales or parallel to the surface. The plane of detachment is located near the stone surface and its thickness is generally from millimeters to centimeters. There are two sub-types of scaling. On one hand, the thin flat or curved scales of thickness lower than 5 millimeters organized as fish scales are called flakes. On the other hand, the scaling in which the scales are parallel to the stone surface are called contour scaling.

In this paper, we propose a semi-automatic technique to identify, measure and map scaling effects on stone surfaces requiring very little interaction by the user. Moreover, we propose a pipeline to process the stone monuments that can be followed by any user without any expert knowledge. Although our technique has some limitations, we consider it as a first step towards an objective stone decay mapping.

2. Previous Work

In **Cultural Heritage** several efforts have been made to better understand the decay of stone in order to develop correct conservation strategies. One of these efforts consists of mapping Visual Weathering forms. This non-destructive method has been widely used in the literature [FHK95] [FHK97] [FHB03].

Since this mapping process is very subjective, it is difficult to have a precise idea of the state of a monument. To solve that Fitzner et al. [FHB00] introduced damage indices as a tool for quantification and rating the stone damages. These indices are based on the area affected and the depth of the loss. In the same line, Warke et al. [WCTS03], tried to simplify the prediction of the behavior of the building stone decay by using the TNM Staging System analogy. This system which uses the depth, area and spread of the decay, helps the conservator to decide if conservation is still possible. Lately, Smith and Prikryl [SP07] examined the medical analogy for stone weathering. They observed the potential of this analogy as it provides understanding of the background of the buildings and they stated the importance of formalizing the condition assessment. More recently, in order to reduce the ambiguity of deterioration mapping, Delgado [Rod15] proposed a new mapping strategy that divides the monument into entities and takes into account its structure to assign a level of priority of restoration.

Lately, some efforts have promoted the use of 3D models in archaeological heritage. De Reu et al. [RPV*13] indicated the limitations of using 2D drawing for weathering mapping and proved that using 3D models is a cost-effective improvement. In a similar line, Stefani et al. [SBJB*14] developed a toolkit that simplified the mapping task. They used a connection between the 3D model and a 2D representation using the NUBES web platform. Finally, Koutsoudis et al. [KVI*14] analyzed the quality of reconstructions of photogrammetry algorithms and they found that high quality results can be achieved if the number of images used is high enough.

Computer Graphics can provide useful tools to reduce the subjectivity of the current mapping methods for weathered stones. Although to the best of our knowledge there is no technique which identifies and maps automatically the decay of stones, there are techniques that try to handle this kind of problem. One approach is to identify and map reliefs and details on surfaces. Zatzarinni et al. [ZTS09] compute the height function over the base without com-

puting the base surface and they use this height to extract relief and details. Similarly, Chen et al. [CCL*11] proposed a technique to visualize and edit reliefs previously extracted by a height threshold from smooth surfaces reconstructed using normal smoothing and Poisson reconstruction. An alternative approach is to analyze the mesh to enhance or recover the features of the models. Kolomenkin et al. [KST08] propose a new class of view-independent curves, which describe places with the strongest inflections on the surface, and they use it to enhance the features during the visualization. With a similar goal, Lawonn et al. [LTPH17] presented a technique to extract carvings on stones. Their algorithm is based on an adaptation of the Frangi filter and an ordering of the detected structures by saliency. They used these structures in the final visualization enhancing the shading of the carvings in the models. Nespeca and De Luca [NDL16]use the point cloud of a wall to obtain quantitative information from the model which they use to guide segmentations and to reconstruct surfaces and volumes. Finally, Peteler et al. [PGB*15] proposed an image-based approach to measure the degradation of a scene using depth maps of the model reconstructed at different time steps.

There are several other techniques of geometrical analysis used in Cultural Heritage. They are mainly focused in collection analysis, interpretation, monitoring, restoration and perception. For a complete review, see Pintus et al. [PPY*16]. Additional related work can be found in computer graphics which synthesizes the effects of weathering on virtual models. For example, Dorsey et al. [DEJ*99] propose a model to compute weathering effects on stone objects using a surface-aligned data structure and a model that simulates changes in the properties and shape of the stones.

3. Overview

The overview of our method is depicted in Figure 1. We start by reconstructing the model using photogrammetry techniques. After that, we need to process the reconstructed scene to isolate the model in a manifold mesh. Then, we apply a preprocessing to the model in order to reduce the typical noise that appears in the reconstruction. We propose using an adaptive anisotropic Gaussian filter. Once the model is processed, we estimate the unweathered surface using a RANSAC technique. In this estimation, we use the point cloud of a segmentation started at a point on an unweathered zone of the surface provided by the user. Then, we perform a geometrical analysis of the curvature of the mesh to find the typical features of scaling weathering effects. Finally, we map the weathered regions using the detected features and an adapted image-space segmentation based on the distance between the mesh and the estimated unweathered surface. This results in a set of weathered regions and features that are classified according to the corresponding sub-type of scaling.

4. Capturing the models

There are several methods to capture a real-world scene and generate a 3D model out of it. Although 3D scanners are able to reconstruct models achieving a very high quality, they are expensive and require trained people to use them. For this reason, photogrammetry techniques are taking a more prominent role. They only require a digital camera and basic training to achieve good results. To simplify the capturing step, thus we use photogrammetry.

Figure 2: *Our method requires an isolated 3D manifold model to work properly. Generating it consists on taking the pictures, loading them to Autodesk Remake, which generates a 3D reconstructed scene and, then, separating the target model and filling its holes.*

We use digital a camera to take a set of pictures around the object. Once all the images are taken, we generate a 3D model from them using Autodesk ReMake. The process consists of loading the pictures to the software and after an automatic process we obtain a 3D reconstruction of the scene. Since our method needs an isolated manifold model to work, we use the provided software tools to remove the parts of the scene not corresponding to the target model and to fill the holes of the unreconstructed parts. Figure 2 illustrates this process. Finally, we calibrate the scale of the reconstructed model using measured distances between points on the real model.

5. Pre-pocessing the models

One inherent problem of the acquisition step is the presence of noise in the reconstruction process, and photogrammetry tends to produce models with noise. Such noise complicates the analysis and understanding of the surface and, consequently, the detection of weathering effects. For this reason it is very important to reduce its presence as much as possible.

Smoothing is a good strategy to reduce noise in a mesh. In general, smoothing techniques use a constant smoothing term over the whole surface which can deform the mesh and remove important information. To avoid that, an adaptive method is needed that preserves the features of the original mesh reducing the noise elsewhere. The challenge is to decide the degree of smoothing at each point. To handle it we perform an adaptive and anisotropic Gaussian filter based on the Ohtake et al. technique [OBS02] to smooth the normals of the mesh. After that, we can use these smoothed normals to subsequently smooth the vertices of the mesh.

First, we compute the best smoothing scale for each face normal

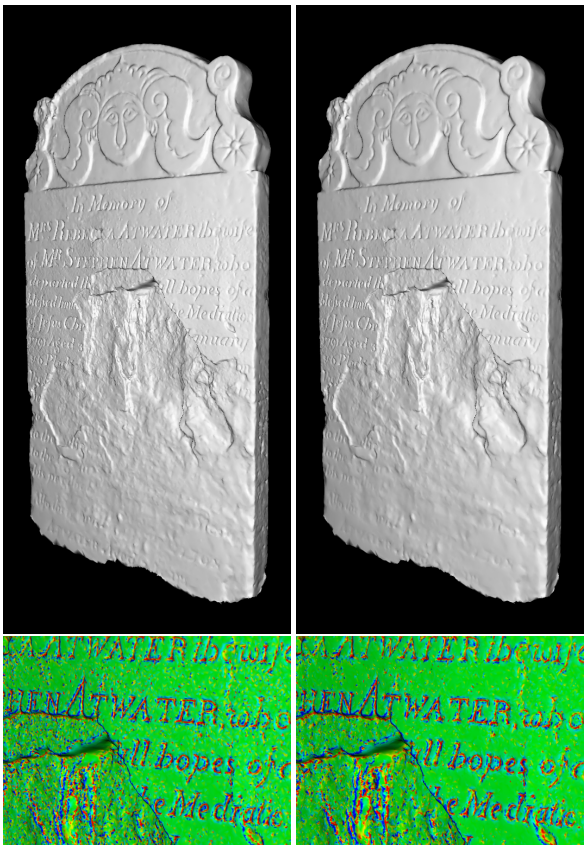

(a) *PreFilter* **(b)** *PostFilter*

Figure 3: *We perform a smoothing filter to reduce the acquisition noise of the reconstructed model. Here it is shown a comparison before and after applying the filter (top) and zoom-in's showing the obtained color-coded curvature in each case (bottom).*

by analyzing the neighboring area. We compute the best standard deviation σ of the Gaussian filter around each normal using the following equation:

$$\sigma_{best} = \arg\min_{\sigma} \frac{c}{\sigma^2} + \varepsilon^2(\sigma) \tag{1}$$

where $c = 4.0 \times 10^{-3} l^2$, l is the arithmetic mean of the edge lengths of the mesh and ε is the local variance of the smoothed normal using a Gaussian filter with a σ standard deviation. To find σ_{best}, we use ten uniformly spaced values of σ from $\sigma_{min} = 0.5l$ to $\sigma_{max} = 5.0l$.

Then, the smoothed normals n'_σ are computed as:

$$n'_\sigma = \frac{\sum w_j n_j}{|\sum w_j n_j|} \tag{2}$$

where n_j are normals of the neighbor triangles at a geodesic distance $d \leq 4\sigma$ and w_j are the weights applied onto the normals which take into account the area of the corresponding triangle and a Gaussian function based on d.

Once the normals of all the faces of the mesh have been smoothed, we smooth the mesh by updating the vertex position as proposed by Sun et al. [SRML07]. According to this, we update each vertex position x' following the equation:

$$x'_i = x_i + \frac{1}{|F_V(i)|} \sum_{k \in F_V(i)} n'_\sigma(k)(n'_\sigma(k) \cdot (C_F(k) - x_i)) \tag{3}$$

where x_i is the original position of the vertex, $F_V(i)$ is the set of surrounding faces of the vertex i, $m_\sigma(k)$ is the smoothed normal of the face k and $C_F(k)$ is the center of the face k. Figure 3 shows the results of applying this smoothing to an example model. We can observe how the level of noise is considerably reduced while the features of the mesh are preserved.

6. Estimating original surface

As mentioned before, the scaling weathering process is characterized by the loss of material on the surface. To be able to detect this loss we first need to estimate the shape of the model before the decay process.

First we detect what parts of the surface have not suffered any weathering. To achieve that, we ask the user to mark a unique point on the surface which has not suffered any weathering process. Taking as input the face where this point lies, we proceed to segment the mesh extending the segmentation taking into account the normal of the face and the already segmented region following the next algorithm:

```
function SEGMENTBASESURFACE(face)
    segmentation ← face
    visitedFaces ← face
    candidates ← face.neighbors()
    meanNormal ← segmentation.meanNormal()
    while !candidates.empty() do
        f ← candidates.pop()
        if !visitedFaces.contains(f) then
            visitedFaces ← visitedFaces ∪ f
            if dot(f.normal(), meanNormal) > threshold then
                segmentation ← segmentation ∪ f
                meanNormal ← segmentation.meanNormal()
                candidates ← candidates ∪ f.neighbors()
    return segmentation
```

Figure 4 (a) shows the result of this segmentation.

Once the base surface is segmented, we use the vertices of the segmented faces to estimate the original surface S_{base}. Although several approaches could be suited to estimate a shape, we use a method based on an efficient RANSAC technique proposed by Schnabel et al. [SWK07]. This method is fast, it handles high levels of noise and it can reconstruct typical hand-made shapes. This technique computes a set of primitive shapes given a point-cloud with its associated normals. At each iteration of their algorithm, the primitive with maximal score is searched using the RANSAC

paradigm: we generate candidates of all the primitive shapes sampling randomly minimal subsets of the point cloud, then we chose the candidate with the highest score and we only accept it if the probability that no better candidate was overlooked during the sampling is high enough.

Figure 4 shows the result of the RANSAC method in the subfigure (b). As the reader can observe, the detected shape does not fit perfectly the original surface S_{base}. This is because although the RANSAC method is able to handle a high percentage of outliers, its recovered surfaces can be shifted for points thatare not on the original surface S_{base}, but not far enough away to be considered outliers.

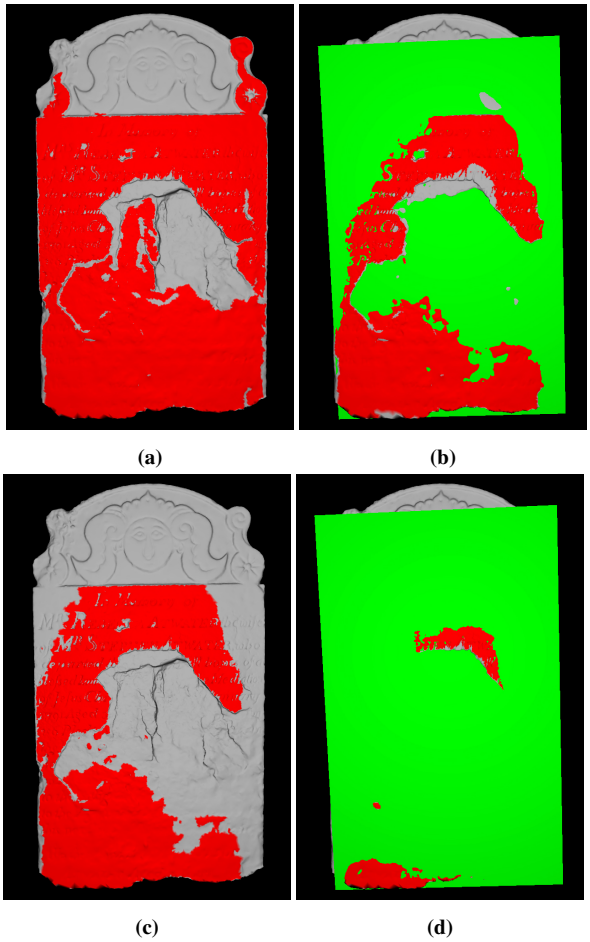

Figure 4: *In order to detect the loss of material in the model, we first need to estimate the corresponding unweathered surface. This is done (a) by performing an initial segmentation starting from an unweathered point marked by the user. Then, we perform a RANSAC process to obtain the unweathered surface estimation (b). This process is iteratively refined removing outliers from segmentation and computing RANSAC again, until no outliers are segmented (c) and the definitive unweathered surface is found (d). We use red color to indicate the segmented faces and green color to show the estimated surface.*

In order to solve that, we propose to use an iterative algorithm where we erase the near outliers from the point cloud. Given a first RANSAC reconstruction, at each iteration we erase the points which are farther than a user defined threshold $\Delta_{outliers}$ and we re-estimate the surface until all the points are inside another user defined threshold $\Delta_{surface}$. The resulting surface S_{base} will be considered as the unweathered surface of the model from this point. This process is described in the following algorithm:

function FINDSURFACE(*pointCloud*)
  repeat
    $shape \leftarrow EfficientRANSAC(pointCloud)$
    $outsiders \leftarrow false$
    for all $p \in pointCloud$ **do**
      if $p.distance(shape) > \Delta_{surface}$ **then**
        $outsiders \leftarrow true$
        break
    if *outsiders* **then**
      for all $p \in pointCloud$ **do**
        if $p.distance(shape) > \Delta_{outliers}$ **then**
          $pointCloud.remove(p)$
  until $outsiders = 0$
  $S_{base} \leftarrow shape$
  return S_{base}

Figure 4 shows the result of this iterative process in subfigure (d) and the last segmentation in subfigure (c). Although the refined segmentation is good enough to be used with RANSAC to estimate the original surface S_{base}, it still selects parts of the weathered region of the model. So, we avoid using it in the next steps of our technique.

7. Detecting weathering

After estimating the original surface S_{base}, we can analyze the differences between the mesh and the reconstructed surface to find loss of material during the scaling weathering process. We propose to classify this process by taking into account the characteristics of the detached regions trying to figure out where the main features are placed and by mapping the affected regions consequently.

7.1. Feature filtering

As mentioned previously, the scaling weathering process is related to the layers of the stone. When the layers fall, they typically show a staircase effect in the margins of the lost area. Moreover, we can use the difference of depth in these staircase steps as an indicator of the subtypes of scaling. For this reason, it is important to detect these steps in the surface.

We propose to use the mean curvature as an indicator of the features of the mesh in order to find such features. First, we compute the mean curvature at the vertices of the mesh. Then, we process this curvature to consider only the vertices where the curvature is maximum or minimum. More specifically, we tag as maximum curvature vertices (CV_{max}) those in which the curvature is greater or equal to the percentile 85. On the other hand, we tag as minimum curvature vertices (CV_{min}), those in which the curvature is lower or equal to the percentile 15. This values give the best results according to our experiments.

Figure 5: *Scaling weathering effects are related to the geometrical features of the model. In order to detect them, we use the mean curvature (left) and we process it taking into account the highest and lowest values and filtering the small features (right).*

We need to find the steps associated with the layers, but since the current approach only takes into account the value of the mean curvature, we can be still considering the remaining noise in the model. To avoid that we propose filtering the noise, untagging all the vertices tagged as minimum or maximum curvature vertices, when the number of connected vertices with the same tag is lower than a user defined threshold tv_{min}. In our experiments, we have seen that setting $tv_{min} = 5$ is enough to achieve good results. This simple idea proved to be very useful to remove the noise while preserving the features where the curvature is minimum and maximum. Figure 5 illustrates it, showing, at left, the mean curvature and, at right, the tagged features after applying the proposed filter.

7.2. Detecting scaling weathering effects

After tagging the features, we can use them to detect the borders of the scaling weathering effects. We can use close features with an opposite tag to detect the typical steps of scaling effects. Moreover, if we analyze the depth differences between the tagged features, we can classify them in the two subtypes of scaling processes.

In order to identify the vertices corresponding to these steps, we propose to go through the tagged vertices and check if there are opposite tagged vertices nearby. We check that by going through the neighbor vertices which are closer than a user defined distance $distance_{feat}$. We compute the distance between two vertices projecting them to the estimated original surface S_{base} and computing the geodesic distance between the projections on that surface. After that, we compute the difference of depth between their two vertices Δ_{depth}. If Δ_{depth} is greater or equal than 0.5cm we consider that the current vertex is part of a scaling weathering feature and, otherwise, we consider it as part of a flake. We use this value after in situ observations taking into account the general tendency of the layers separation. Our values apply to the sandstone we are examining, but can be adapted to other types of stone. Our classification is not exclusive, some vertices can be considered part of a scaling and of a flake. A reason for that could be the presence of flakes on a scaling weathering step. Moreover, in our experiments we have observed that setting $distance_{feat} = 1$cm is enough to detect most of the features. This process is described more specifically in the following algorithm:

function CLASSIFYSCALINGVERTICES($vertices, S_{base}$)
  for all $v \in vertices$ **do**
    $v_{proj} \leftarrow S_{base}.projection(v)$
    $candidates \leftarrow v.neighbors()$
    for all $c \in candidates$ **do**
      $c_{proj} \leftarrow S_{base}.projection(c)$
      $dist_{v,c} \leftarrow S_{base}.geodesicDistance(v_{proj}, c_{proj})$
      if $dist_{v,c} \leq distance_{feat}$ **then**
        $candidates \leftarrow candidates \cup c.neighbors()$
        if $(v \in CV_{max} \wedge c \in CV_{min}) \vee$
         $(v \in CV_{min} \wedge c \in CV_{max})$ **then**
          $depth_v \leftarrow S_{base}.distance(v)$
          $depth_c \leftarrow S_{base}.distance(c)$
          $depth_{v,c} \leftarrow abs(depth_v - depth_c)$
          if $depth_{v,c} \geq \Delta_{depth}$ **then**
            $v.scaling \leftarrow true$
          else
            $v.flaking \leftarrow true$

Figure 6 shows the resulting classification of vertices as part of scaling weathering processes using the filtered features shown in Figure 5. The color code of the vertices is the following: red for the flakes, green for the scaling and yellow for the vertices that are part of weathering scales and flakes.

7.3. Segmentation of weathered regions

At this point, we are able to detect the vertices that belong to the typical steps of the scaling weathering processes and we are even able to classify them in subtypes. But, we are not yet able to map the regions of the surface affected by this weathering effect as it is traditionally done in Cultural Heritage. Mapping the regions is important because it gives us the information about the area affected and its spread.

To solve that we propose segmenting the surface in regions by adapting the image-based segmentation approach of Felzenszwalb and Huttenlocher [FH04]. The authors measure the evidence for a boundary between two regions using a graph-based representation of the image. The edges of the graph are assigned with a weight that measures the dissimilarity between neighbors. Then, they join regions of the image if a boundary is not found. A boundary appears when the minimum weight between the elements of the border of both regions is higher than the minimum internal weight between the elements of each region. This simple predicate results in a fast solution that preserves the features of the images.

In our case, we have a 3D mesh instead of a 2D image, and we are interested in segmenting regions based on depth rather than color. For this, we represent each surface point in terms of its distance to the original unweathered surface S_{base}, resulting in a depth map over this surface. Then, we generate a 2D image of this depth

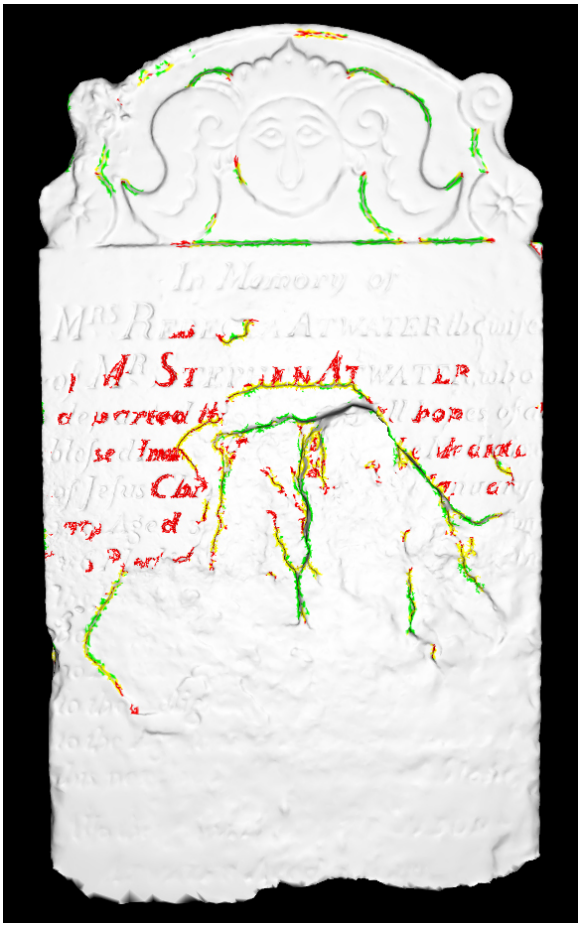

Figure 6: *In order to identify the sub-types of scaling effects present on the model, our technique analyzes the vertices previously detected as features related to the scaling effect. It classifies them depending if they form part of flakes (red), weathering scales (green) or both of them (yellow), using the difference of depth with respect to the unweathered surface and its neighbors.*

map using a direct parametrization, and we use this map as input to the segmentation algorithm.

Figure 7, at left, shows an example of depth image used as input to the image segmentation algorithm and, at right, the resulting segmentation. As can be observed, this depth-based segmentation follows the main characteristics of the model shape.

7.4. Mapping the regions

At this point, we have all the information needed to map the scaling weathering effect onto the model. First, we need to process the segmentation of the surface to discard the segmented regions of the unweathered parts. To achieve that, we perform a culling of the segmented regions taking into account their distance to the estimated unweathered surface (S_{base}). Such distance is computed as

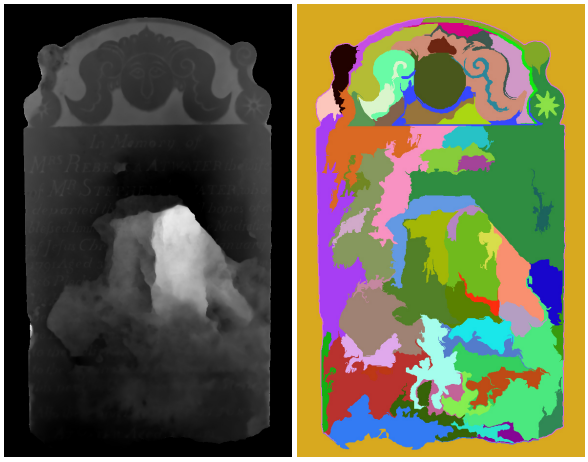

Figure 7: *In order to detect regions affected by the scaling weathering effect, we first need to identify the different regions of the model. Our region segmentation uses a map of the distance between the model and the estimated unweathered surface (left) and computes the region segmentation in image-space (right).*

the mean depth ($depth_{mean}$) of all the points inside of each region (R). We define this culling process following this rule:

$$Culling(R) = \begin{cases} true, & \text{if } S_{base}.distance(p_{mean}) < dist_{min} \\ false, & \text{otherwise} \end{cases} \quad (4)$$

where $dist_{min}$ is a user defined threshold. This culling process takes into account the segmented regions instead of evaluating each point individually, thus avoids considering as weathered region most of the carvings of the model (which fall on regions whose mean distance is under $dist_{min}$).

After that, we propose tagging the segmented regions which have not been discarded during the culling taking into account the identification of the scaling vertices described in Section 7.2. In this way, for each region we check if the vertices inside that region have detected scaling and which of the possible sub-types. We define this tagging of each region (R) following this rule:

$$Tagging(R) = \begin{cases} Scaling, & \text{if } \forall v \in R : v \in \mathcal{C}_s \vee v \in \mathcal{C}_u \\ Flaking, & \text{if } \forall v \in R : v \in \mathcal{C}_f \vee v \in \mathcal{C}_u \\ Both, & \text{if } \exists v \in R : v \in \mathcal{C}_b \\ Unknown, & \text{otherwise} \end{cases} \quad (5)$$

where $\mathcal{C}_s$ is the set of vertices that are tagged only as scaling, $\mathcal{C}_f$ is the set of vertices tagged only as flaking, $\mathcal{C}_b$ is the set of vertices that are tagged as flaking and scaling, and $\mathcal{C}_u$ is the set of untagged vertices.

Figure 8 illustrates the result of the culling process applied to the segmentation showed at Figure 7 (left) and the final classification of this segmented regions (right). The regions where we only detect scaling are displayed in green, the regions where we detect flaking

Model	#Pictures	#Triangles	Smoothing (s)	Unweathered surface (s)	Scaling features (s)	Map regions (s)
1	188	201K	181.50	0.13	2.12	4.89
2	165	193K	237.87	0.28	2.75	4.91
3	166	427K	612.42	23.97	5.73	4.94
4	123	173K	157.52	0.88	2.03	4.73
5	214	167K	168.68	4.36	1.97	4.83

Table 1: *Performance of our technique for different models. For each model, we show the number of pictures used in the reconstruction, the number of triangles of the reconstructed 3D model and the performance in seconds of each step of our technique: smoothing the model (Section 5), estimating the unweathered surface (Section 6), detecting the scaling weathering features (Sections 7.1 and 7.2) and mapping the weathered regions (Sections 7.3 and 7.4).*

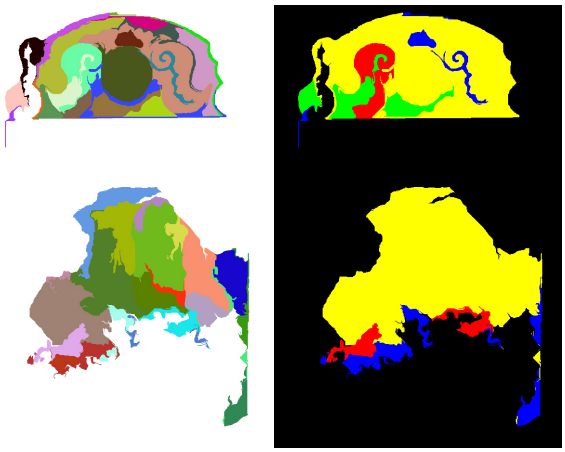

Figure 8: *From the previously detected regions on the model, we need to discard those close to the unweathered surface. We perform this culling taking into account the mean distance of each region to the estimated unweathered surface (left). Then, taking into account the scaling weathering features, we tag the surviving regions according to the sub-type of scaling effect present on them (right).*

are in red, the regions with both effects are shown in yellow and, finally, the regions where we found detachment but they are not tagged with any type of scaling are colored blue.

8. Results and Discussion

We have tested our approach on different models. We have reconstructed all of them with the same setup. We used a Nikon D7000 digital camera mounted on a tripod, with a fixed lens with a focal length of 18mm. We took pictures at maximum resolution (4928x3264). Table 1 shows the characteristics of the models and the performance we obtain, for an unoptimized code, on a MacBook Pro 15" with an Intel Core i7 2.6GHz, 16GB memory and a NVIDIA GeForce GT 750M with 2GB memory. We have used large sets of pictures to get models with enough quality. Despite the number of triangles, most of the processes are performed in seconds. The smoothing of the mesh takes some minutes, but is only computed once.

Figure 9 shows the potential of our technique. It is formed by a set of comparisons between the results of our technique and the mapping performed by an expert in Cultural Heritage. The top row of the figure shows the original reconstructed models with its original texture. In the middle row, we show the model with the mapping of the detected weathering. The weathered regions mapping (see Section 7.4) is blended with the original color to help the viewer to judge our mapping. Moreover, the weathering features (see Section 7.2) are highlighted to provide extra information to the user. Finally, bottom row corresponds to the mapping performed by the expert. In middle and bottom rows, we have used the same color code: green for scaling, red for flaking, yellow for the zones where there is scaling and flaking and blue for the detached regions where there is no scaling/flaking process.

We think our approach represents a first step forward in the mapping of weathering effects. It represents a new tool which is able to reduce the ambiguity and subjectivity of the current mapping procedures. Moreover, our approach is suitable for all kind of users. Once the user has taken the pictures and reconstructed the model, our technique only requires a single click on an unweathered region and the adjustment of some intuitive thresholds to perform an automatic analysis and segmentation. Furthermore, our proposed pipeline is independent of the reconstruction method and it can be used with LIDAR data, for instance. Although we have tested our method only in grave markers with flat shapes, it can be extended to all the forms supported by RANSAC: planes, cylinders, spheres, cones and tori. Fortunately, as a result of being man-made, many ancient monuments and buildings can be decomposed in these shapes. In that case, the normals similarity strategy used in Section 6 should be adapted appropriately. Moreover, we will need a 2D parametrization of the shape to obtain a distance image,which is necessary for the segmentation of the weathered regions.

In Figure 9, it is possible to see how our technique is very good detecting the weathering regions and isolating them from the unweathered surface, even if it contains inscriptions or superficial carvings (see subfigure (c)). It can detect weathered regions of multiple degrees and the region segmentation is very useful to divide them in different entities (see subfigure (a), central hole of (c), upper part of (d) and main holes of (c)). Moreover, in many cases, the presented technique is able to classify these weathered regions into the different scaling sub-types thanks to the feature analysis (see subfigure (c), (c) central hole and (e) upper holes). There are cases where the classification differs considerably between our technique and the expert mapping (see subfigure (a) and (d)). This is caused

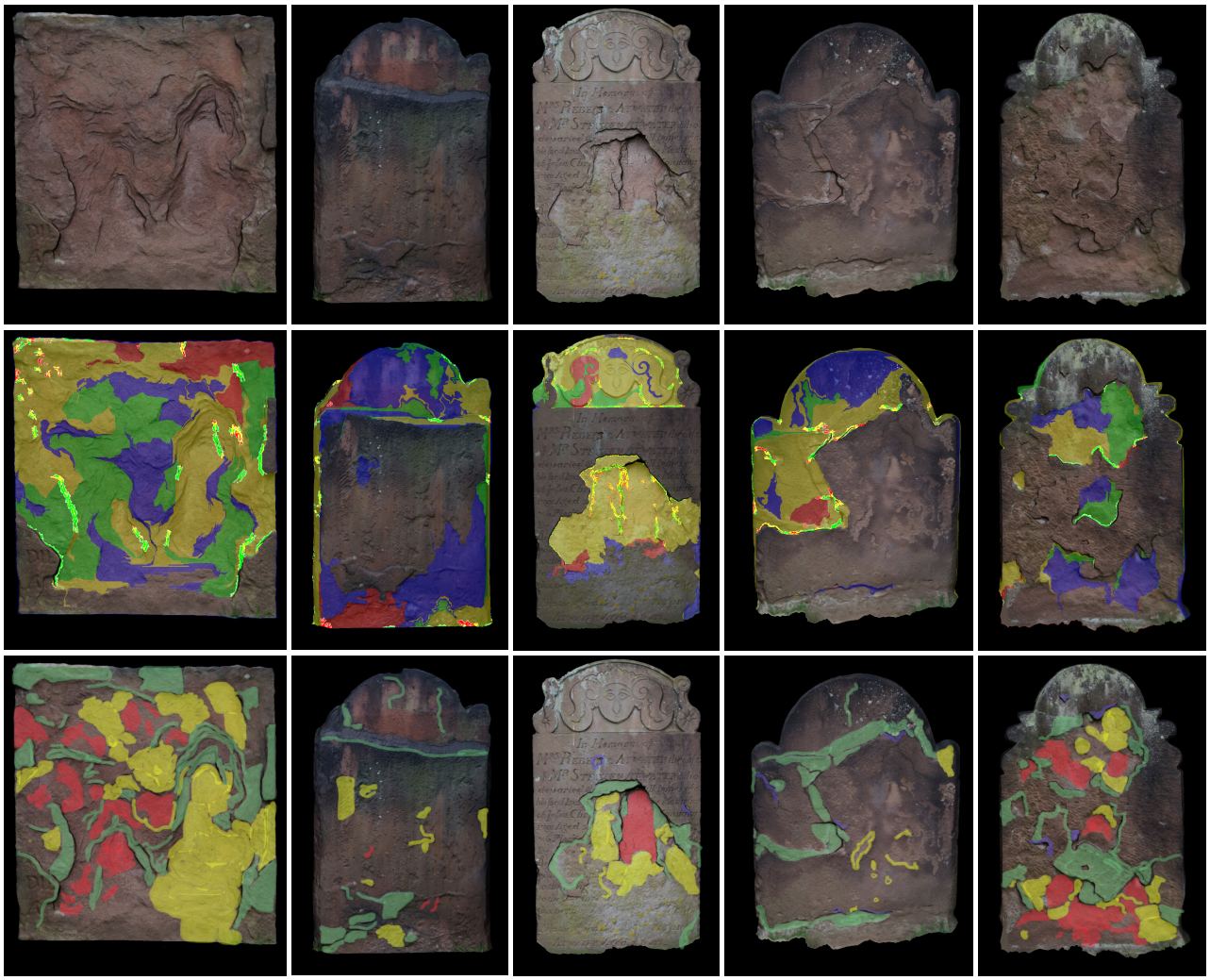

(a) *Model 1* **(b)** *Model 2* **(c)** *Model 3* **(d)** *Model 4* **(e)** *Model 5*

Figure 9: *Results of our method (middle) for different reconstructed models (top) compared to a mapping of an expert in Cultural Heritage (bottom). The color-code of the weathering regions describes the corresponding sub-type of scaling weathering effect. It is red for flaking, green for scaling, yellow for both and blue for detachments which we are not able to classify in a specific sub-type. The width of these models are in the range formed by 57cm for Model 2 and 85cm for Model 1.*

by the expert subjectivity and differences in feature classification. Finally, the highlighting of these features during visualization provides an interesting tool for user inspection to uncover subtle features.

Our method also has some limitations. It can be misled by deep carvings and sculpture reliefs, and it can map them as weathered regions of the surface (see Figure 9 (c) top and (b) margins). Although some techniques to try to detect these regions can be applied to identify and reduce this problem, we think that these cases are simple enough to detect for a user and they can be removed with some simple interaction. Another limitation of our technique is that the mapping procedure can skip weathered regions if they are small and not deep enough (see Figure 9 (b)(d) unweathered surface). This is caused by how the image-space depth segmentation computes the borders and it is more noticeable if the model has large and deep weathered zones. In that case, avoiding small detached zones is a problem of low incidence if we consider the whole model. Finally, our technique is dependent on the initial reconstruction. If its surface is not able to represent the features of the surface our technique will not be able to detect the scaling features (see Figure 9 (a) small features). In addition, as our technique consists of several independent steps there is the possibility that the error of each step is accumulated in the final result. For these reasons, our technique performs better with large sets of pictures with high resolution.

9. Conclusions and Future Work

We have introduced a technique to detect weathering effects on stone monuments. From an easy to perform 3D reconstruction of a model, we are able to analyze its geometry and to identify and map the features and characteristics of scaling weathering effects. Moreover, we are able to detect two sub-types of scaling and to represent them on the mapping. Our technique has the advantage of requiring little interaction from the user to isolate well the weathered region from the surface. Although our method has some limitations, current manual mapping also has its own limitations. By contrast, the presented method is a first big step towards the reduction of ambiguity and subjectivity of manual maps. We think that this technique can open a new line to improve the mapping and tracing of weathering effects in Cultural Heritage conservation projects.

In the future, we would like to extend our work to make it handle all the shapes detected by RANSAC. This will open up the opportunity to apply our technique to a broader range of monuments and buildings. Moreover, we would like to incorporate the detection of other weathering characteristics like volume loss, area of the loss and spread of it, in order to be able to compute the damage indices and the medical analogies described in the literature. Finally, we would like to improve the current tagging of the regions using an statistical analysis with a temperature map of confidence.

10. Acknowledgements

This work was partially funded by TIN2014-52211-C2-2R project from Ministerio de Economía y Competitividad (Spain) and by MPCUdG2016/125 project from Universitat de Girona (Spain).

References

[CCL*11] CHEN Y., CHENG Z.-Q., LI J., MARTIN R. R., WANG Y.-Z.: Relief extraction and editing. *Computer-Aided Design 43*, 12 (2011), 1674–1682. 3

[DEJ*99] DORSEY J., EDELMAN A., JENSEN H. W., LEGAKIS J., PEDERSEN H. K.: Modeling and rendering of weathered stone. *ACM Transaction on Graphics (Proc. SIGGRAPH)* (1999), 225–234. 3

[FH04] FELZENSZWALB P. F., HUTTENLOCHER D. P.: Efficient graph-based image segmentation. *International Journal of Computer Vision 59*, 2 (2004), 167–181. 6

[FHB00] FITZNER B., HEINRICHS K., BOUCHARDIERE D. L.: Damage index for stone monuments. In *Protection and Conservation of the Cultural Heritage in the Mediterranean Cities: Proceedings of the 5th International Symposium* (2000), pp. 315–326. 2

[FHB03] FITZNER B., HEINRICHS K., BOUCHARDIERE D. L.: Weathering damage on pharaonic sandstone monuments in Luxor-Egypt. *Building and Environment 38*, 9-10 (2003), 1089–1103. Building Stone Decay: Observations, Experiments and Modeling. 2

[FHK95] FITZNER B., HEINRICHS K., KOWNATZKI R.: Weathering forms - classification and mapping. In *Denkmalpflege und Naturwissenschaft, Natur- steinkonservierung* (1995), pp. 41–88. 2

[FHK97] FITZNER B., HEINRICHS K., KOWNATZKI R.: Weathering forms at natural stone monuments - classification, mapping and evaluation. 105–124. 2

[ICO08] ICOMOS: *Monuments and Sites XV - Illustrated glossary on deterioration patterns*. ICOMOS International Scientific Committee for Stone, 2008. 1

[KST08] KOLOMENKIN M., SHIMSHONI I., TAL A.: Demarcating curves for shape illustration. *ACM Transaction on Graphics (Proc. SIGGRAPH Asia) 27*, 5 (Dec. 2008), 157:1–157:9. 3

[KVI*14] KOUTSOUDIS A., VIDMAR B., IOANNAKIS G., ARNAOUTOGLOU F., PAVLIDIS G., CHAMZAS C.: Multi-image 3D reconstruction data evaluation. *Journal of Cultural Heritage 15*, 1 (2014), 73–79. 2

[LTPH17] LAWONN K., TROSTMANN E., PREIM B., HILDEBRANDT K.: Visualization and extraction of carvings for heritage conservation. *IEEE Transactions on Visualization and Computer Graphics 23*, 1 (2017), 801–810. 3

[NDL16] NESPECA R., DE LUCA L.: Analysis, thematic maps and data mining from point cloud to ontology for software development. In *The International Archives of the Photogrammetry, Remote Sensing and Spatial Information Sciences* (2016), vol. XLI-B5 of *XXIII ISPRS Congress*, pp. 347–354. 3

[OBS02] OHTAKE Y., BELYAEV A., SEIDEL H.-P.: Mesh smoothing by adaptive and anisotropic gaussian filter applied to mesh normals. In *vision modeling and visualization* (2002). 3

[PGB*15] PETELER F., GATTET E., BROMBLET P., GUILLON O., VALLET J. M., LUCA L. D.: Analyzing the evolution of deterioration patterns: A first step of an image-based approach for comparing multitemporal data sets. In *2015 Digital Heritage* (Sept 2015), vol. 2, pp. 113–116. 3

[PPY*16] PINTUS R., PAL K., YANG Y., WEYRICH T., GOBBETTI E., RUSHMEIER H.: A survey of geometric analysis in cultural heritage. *Computer Graphics Forum 35*, 1 (2016), 4–31. 3

[Rod15] RODRIGUES J. D.: Defining, mapping and assessing deterioration patterns in stone conservation projects. *Journal of Cultural Heritage 16*, 3 (2015), 267–275. 2

[RPV*13] REU J. D., PLETS G., VERHOEVEN G., SMEDT P. D., BATS M., CHERRETTÃL' B., MAEYER W. D., DECONYNCK J., HERREMANS D., LALOO P., MEIRVENNE M. V., CLERCQ W. D.: Towards a three-dimensional cost-effective registration of the archaeological heritage. *Journal of Archaeological Science 40*, 2 (2013), 1108–1121. 2

[SBJB*14] STEFANI C., BRUNETAUD X., JANVIER-BADOSA S., BECK K., LUCA L. D., AL-MUKHTAR M.: Developing a toolkit for mapping and displaying stone alteration on a web-based documentation platform. *Journal of Cultural Heritage 15*, 1 (2014), 1–9. 2

[SP07] SMITH B. J., PRIKRYL R.: Diagnosing decay: the value of medical analogy in understanding the weathering of building stones. *Geological Society, London, Special Publications 271* (2007), 1–8. 1, 2

[SRML07] SUN X., ROSIN P., MARTIN R., LANGBEIN F.: Fast and effective feature-preserving mesh denoising. *IEEE Transactions on Visualization and Computer Graphics 13*, 5 (2007), 925–938. 4

[SWK07] SCHNABEL R., WAHL R., KLEIN R.: Efficient RANSAC for point-cloud shape detection. *Computer Graphics Forum 26*, 2 (2007), 214–226. 4

[WCTS03] WARKE P., CURRAN J., TURKINGTON A., SMITH B.: Condition assessment for building stone conservation: a staging system approach. *Building and Environment 38*, 9-10 (2003), 1113–1123. Building Stone Decay: Observations, Experiments and Modeling. 1, 2

[ZTS09] ZATZARINNI R., TAL A., SHAMIR A.: Relief analysis and extraction. *ACM Transactions on Graphics (Proc. SIGGRAPH Asia) 28*, 5 (Dec. 2009), 136:1–136:9. 2